

Effects Of Entrance Region Transport Processes On Slip Flow Regime In A Wavy Wall Microchannel With Isothermally Heated Walls

H. Shokouhmand, S. Bigham

Abstract— In this study, thermal and hydrodynamic characters of a hydrodynamically and thermally developing flow in a wavy microchannel are analyzed. A numerical simulation has been carried out to solve the continuum, momentum and energy equations in curvilinear coordinate. The equations are discretized using the finite-volume method on a staggered mesh and solved by SIMPLE algorithm. A fully implicit scheme is used for the temporal terms and the hybrid differencing is applied for the approximation of the convective terms. Maxwell slip condition and Von-Smoluchowski's temperature jump boundary condition are imposed. The effect of rarefaction on thermal and hydrodynamic characters of flow in wavy microchannels is explored. Also the effect of creep flow is assumed. The results show that Knudsen number has an important effect on both the $C_f \cdot Re$ and Nusselt number on the undeveloped fluid flow. To verify the code a comparison is carried out with available results and good agreement is achieved.

Index Terms— Wavy Wall Microchannel, Slip Conditions, Entrance Region, FVM Method

I. INTRODUCTION

In the past decade, investigation of micro-scale flows has become more and more important due to their wide application in electronic equipments, heat exchangers, sensors and flow controls, reactors, power systems and microelectromechanical systems (MEMS). One of the important goals related to micro thermal devices is the removal of a large amount of dispersed heat from a small space. So, the existences of accurate and efficient analysis are very important to achieve this goal.

Flow in wavy channels has had wide application because of increasing the rate of heat transfer. This advantage might become more important in micro-scale devices. In spite of this important advantage, according to the knowledge of authors, there are a few investigations into wavy channels in micro-scale. The hydrodynamic and thermal characteristics of flow in microchannels in the simple geometries have been studied by many researchers though [1]–[4].

Based on the magnitude of Knudsen number ($Kn = \lambda/L^*$,

the ratio between the gas mean free path and the length scale) fluid flows exhibit different behaviors. Therefore, some classifications have been done. According to the magnitude of Knudsen number flows are divided into four regimes: continuum, slip, transition and free molecular flows. In microchannels due to the minute length scale, the Knudsen number gets a significant value and it determines the behavior of fluid flow. In this work, the slip regime is studied and the Knudsen number is in the range from 0.001 to 0.1. Different investigations on the microchannel heat transfer in this regime have been carried out [5]–[7]. In this regime, velocity slip and temperature jump occur at the wall surface and thereby, flow characteristics such as Nusselt number and $C_f \cdot Re$ are influenced. Theoretical and numerical studies within the slip flow regime typically use the Navier–Stokes approach model and energy equation along with appropriate slip wall and temperature jump models.

In the past decade, considerable efforts have been devoted to analyze fluid flow and heat transfer in wavy channels and microchannels. Cheng [8] studied a family of locally constricted channels, and in each case, the shear stress at the wall was found to be sharply increased at and near the region of constriction. Vradis et al. [9] studied the steady, two-dimensional case in channel in curvilinear orthogonal and non-orthogonal coordinate systems. They illustrated that the vorticity remains constant in the straight section of the channel close to the inlet, increasing rapidly as the wall starts converging. Also it was shown that the vorticity peaks at the point where the cross-sectional area becomes minimum and drops rapidly as the flow enters the diverging part of the channel. Wang et al. [10] numerically studied forced convection in a symmetric wavy wall macro channel. Their results showed that the amplitudes of the Nusselt number and the skin-friction coefficient increase with an increase in the Reynolds number and the amplitude–wavelength ratio. The heat transfer enhancement is not significant at smaller amplitude wavelength ratio; however, at a sufficiently larger value of amplitude wavelength ratio the corrugated channel will be seen to be an effective heat transfer device, especially at higher Reynolds numbers. Arkilic et al. [11] investigated helium flow through microchannels. It is found that the pressure drop over the channel length was less than the continuum flow results. The friction coefficient was only about 40% of the theoretical values. Beskok et al. [12] studied the rarefaction and compressibility effects in gas microflows in the slip flow regime and for the Knudsen number below 0.3. Their formulation is based on the classical Maxwell/Smoluchowski boundary conditions that allow

Manuscript received November 25, 2009. The 2010 International Conference of Mechanical Engineering (ICME'10)

H. Shokouhmand, distinguished professor of Mechanical Engineering, College of Engineering, University of Tehran, Tehran, Iran (corresponding author to provide phone: +982188005677; Fax: +982188013029; e-mail: hshokoh@ut.ac.ir).

S. Bigham, M.Sc. student of Mechanical Engineering, College of Engineering, University of Tehran, Tehran, Iran (e-mail: sajjadbigham@gmail.com).

partial slip at the wall. It was shown that rarefaction negates compressibility. They also suggested specific pressure distribution and mass flow rate measurements in microchannels of various cross sections.

Although the hydrodynamic and thermal aspects of fluid flow in normal microchannels have been extensively studied, to the best of the author's knowledge, the fluid/thermal analysis of wavy microchannel has never reported. The present work is an attempt to fill the literature gap in this regard.

II. FORMULATION OF THE PROBLEM

To begin with, Fig. 1 shows the geometry of interest which is seen to be a two-dimensional symmetric wavy channel. The channel walls are assumed to extend to infinity in the z-direction (i.e., perpendicular to the plane). The mathematical non-dimensional expression of wavy wall is given as

$$y_w(x) = 0.5 + a(1 - \sin(2\pi(\frac{x}{\lambda} - 0.125))) \quad (1)$$

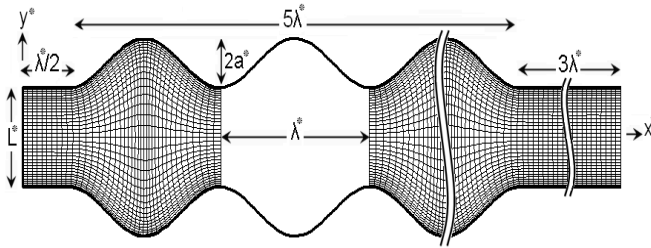


Fig 1 Physical domain of wavy microchannel

Steady laminar flow with constant properties is considered. The present work is concerned with both thermally and hydrodynamically developing flow cases. In this study the usual continuum approach is coupled with two main characteristics of the micro-scale phenomena, the velocity slip and the temperature jump. A general non-orthogonal curvilinear coordinate framework with (ξ, η) as independent variables is used to formulate the problem. The non-dimensional governing equations can be written as:

Continuity:

$$\frac{\partial U^C}{\partial \xi} + \frac{\partial V^C}{\partial \eta} = 0 \quad (2)$$

X-momentum:

$$\begin{aligned} \frac{\partial}{\partial \xi}(uU^C) + \frac{\partial}{\partial \eta}(uV^C) &= \frac{1}{Re_i} \left\{ \frac{\partial}{\partial \xi}(q_{11} \frac{\partial u}{\partial \xi}) \right. \\ &+ \frac{\partial}{\partial \eta}(q_{22} \frac{\partial u}{\partial \eta}) + \frac{\partial}{\partial \xi}(q_{12} \frac{\partial u}{\partial \eta}) + \frac{\partial}{\partial \eta}(q_{12} \frac{\partial u}{\partial \xi}) \left. \right\} \\ &- \frac{\partial}{\partial \xi}(y_\eta p) + \frac{\partial}{\partial \eta}(y_\xi p) \end{aligned} \quad (3)$$

Y-momentum:

$$\begin{aligned} \frac{\partial}{\partial \xi}(vU^C) + \frac{\partial}{\partial \eta}(vV^C) &= \frac{1}{Re_i} \left\{ \frac{\partial}{\partial \xi}(q_{11} \frac{\partial v}{\partial \xi}) \right. \\ &+ \frac{\partial}{\partial \eta}(q_{22} \frac{\partial v}{\partial \eta}) + \frac{\partial}{\partial \xi}(q_{12} \frac{\partial v}{\partial \eta}) + \frac{\partial}{\partial \eta}(q_{12} \frac{\partial v}{\partial \xi}) \left. \right\} \\ &+ \frac{\partial}{\partial \xi}(x_\eta p) - \frac{\partial}{\partial \eta}(x_\xi p) \end{aligned} \quad (4)$$

Energy:

$$\begin{aligned} \frac{\partial}{\partial \xi}(\theta U^C) + \frac{\partial}{\partial \eta}(\theta V^C) &= \frac{1}{Pe_i} \left\{ \frac{\partial}{\partial \xi}(q_{11} \frac{\partial \theta}{\partial \xi}) \right. \\ &+ \frac{\partial}{\partial \eta}(q_{22} \frac{\partial \theta}{\partial \eta}) + \frac{\partial}{\partial \xi}(q_{12} \frac{\partial \theta}{\partial \eta}) + \frac{\partial}{\partial \eta}(q_{12} \frac{\partial \theta}{\partial \xi}) \left. \right\} \end{aligned} \quad (5)$$

where :

$$\begin{aligned} U^C &= uy_\eta - vx_\eta, \quad V^C = -uy_\xi + vx_\xi \\ J &= x_\xi y_\eta - x_\eta y_\xi, \quad q_{11} = \frac{1}{J}(y_\eta^2 + x_\eta^2) \\ q_{12} &= \frac{-1}{J}(x_\xi x_\eta + y_\xi y_\eta), \quad q_{22} = \frac{1}{J}(x_\xi^2 + y_\xi^2) \end{aligned}$$

u, v are the physical velocity components and U_c and V_c are the velocities in ξ, η coordinates, respectively. Here, θ represents non-dimensional temperature. The employed dimensionless variables are defined as follows:

$$x = \frac{x^*}{L^*}, \quad y = \frac{y^*}{L^*}, \quad p = \frac{p^*}{\rho u_i^{*2}}, \quad u = \frac{u^*}{u_i^*}$$

$$v = \frac{v^*}{u_i^*}, \quad Re_i = \frac{\rho u_i^* L^*}{\mu}, \quad Pe_i = Re_i Pr = \frac{u_i^* L^*}{\alpha}$$

$$\theta = \frac{T - T_i}{T_w - T_i}$$

Here, u_i^* and T_i are the inlet velocity and inlet temperature, respectively.

III. SLIP FLOW EFFECTS AND BOUNDARY CONDITIONS

In order to estimate the slip effect at wall under rarified condition, the Maxwell slip condition has been widely used which is based on the first-order approximation of wall-gas interaction from kinetic theory of gases [13, 14]. The magnitude of tangential accommodation coefficient expresses the degree of non-elastic diffusive reflection between gas molecules and wall molecules [15]. Using Von-Smoluchowski's model we have the following boundary conditions at wall in curvilinear coordinate form:

$$\begin{aligned} U_s &= \frac{2 - \sigma_v}{\sigma_v} Kn_i \frac{\partial U_s}{\partial n} \Big|_w + \frac{3}{2\pi} \frac{(1 - \gamma) Kn_i^2 Re_i}{\gamma Ec_i} \frac{\partial \theta}{\partial s} \Big|_w \\ \theta_s &= 1 - \left(\frac{2 - \sigma_T}{\sigma_T} \right) \left(\frac{2\gamma}{\gamma + 1} \right) \frac{Kn_i}{Pr_i} \frac{\partial \theta}{\partial n} \Big|_w \end{aligned} \quad (6)$$

where γ and σ represent the specific heat ratio and accommodation coefficient, respectively. The second term in the slip velocity associates with the thermal creep.

Here, Ec_i means the Eckert number which is defined as

$$Ec_i = \frac{u_i^{*2}}{c_p (T_w - T_i)} \quad (7)$$

where, Pr and Kn mean the Prandtl number and Knudsen number, respectively. The Knudsen number shows the effect of rarefaction on flow properties. A nonzero Knudsen number means a slip flow with nonzero flow velocity at the boundaries and nonzero temperature difference between the boundaries and adjacent flow. In the present work, the slip flow regime with the Knudsen number ranging from 0.01 to 0.1 is considered.

Also in this work, the study is limited to incompressible flow. The flow can be considered incompressible for Mach number lower than 0.3 [16].

Moreover, the other boundary conditions should be defined. A uniform inlet velocity and temperature are specified as

$$u = 1, v = 0, \theta = 0 \quad (8)$$

In the outlet, fully developed boundary conditions are assumed as

$$\frac{\partial u}{\partial x} = \frac{\partial v}{\partial x} = \frac{\partial \theta}{\partial x} = 0 \quad (9)$$

Also the friction coefficient and Nusselt number for a hydrodynamically-thermally developing flow in the wavy micro channel are calculated by,

$$C_f Re = \frac{4(y_w(x))^2}{\left(\int u(x, y) dy\right)^2} \frac{\partial u^{tang}(x)}{\partial n} \quad (10)$$

$$Nu = \frac{1}{\theta_{ave}(x) - 1} \frac{\partial \theta(x)}{\partial n} \Big|_w \quad (11)$$

IV. VALIDATION OF NUMERICAL CODE

In Fig. 2, a comparison with the previously published result of Wang and Chen [10] is carried out to validate the numerical code and non-orthogonal grid discretization scheme of the present study. Their model is analogous to the present model but with the water as working fluid and macro scale channel. Also there is no slip effect with fixing Kn number at zero.

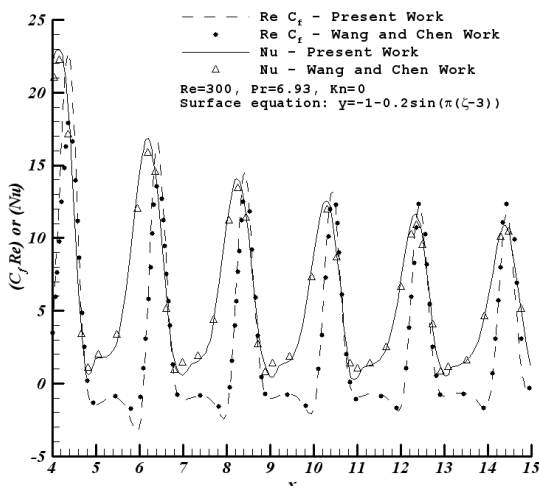


Fig. 2 Validation of the numerical code with available results

V. GRID INDEPENDENCY

The resulting numerical velocity and temperature fields may be used to calculate $C_f Re$ and Nu along the length of the microchannel. The accuracy of the numerical solutions and the time required to reach a solution are dependent on the grid resolution. In this paper, all computations are performed on three grids comprising 550×65, 600×75 and 650×85 control volumes respectively. The obtained results showed sufficient accuracy on these range of grid resolutions. For instance, this accuracy is indicated for Nu along the microchannel with the conditions specified in Fig. 3. Grid dependence studies have been completed with similar results for each numerical solution presented in the results section. Hence, for simplicity all subsequent results presented in result section are obtained using 600×75 grid.

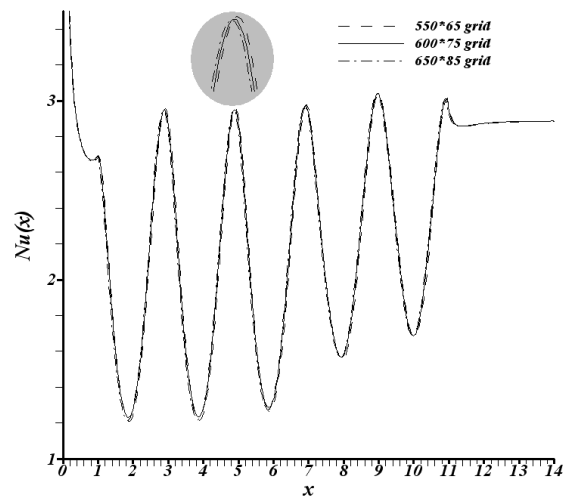


Fig. 3 Numerical results of local Nusselt number along the wavy microchannel with KN=0.075 at Re=2 and a=0.2

VI. SOLUTION PROCEDURE

The governing equations with appropriate boundary conditions are solved by employing the SIMPLE algorithm [17], a finite volume method, in non-orthogonal curvilinear coordinate framework. A fully implicit scheme is used for the temporal terms and the HYBRID differencing [18] is applied for the approximation of the convective terms. The Poisson equations is solved for (x, y) to find grid points [19] and are distributed in a non-uniform manner with higher concentration of grids close to the curvy walls and normal to all walls, as shown in Fig. 1. In this work, a full-staggered grid is used. The discrete form of the momentum and energy equations and all the boundary conditions are obtained by applying a second order central difference scheme. While for boundary nodal points, the one-way difference scheme is applied (i.e., forward for lower and inlet boundaries and backward for upper and outlet boundaries).

One convergence criteria is a mass flux residual less than 10^{-8} for each control volume. Another criteria that is established for the steady state flow is $(|\phi_{i+1} - \phi_i|/|\phi_{i+1}|) \leq 10^{-10}$ where ϕ represents any dependent variable, namely u, v and θ , and i is the number of iteration.

VII. RESULTS AND DISCUSSION

In this section, the results of computer program based on the mathematical model developed in the previous sections are presented. The velocity field, local temperature field, friction factor and local Nusselt number through the wavy microchannel are exhibited. To reduce the computation work, only one half of microchannel, shown in Fig. 1, is considered due to the symmetrical conditions. However, the results presented in the results section are shown for the whole microchannel. The boundaries are maintained at temperature $T_w=70^\circ\text{C}$ and the uniform inlet temperature is considered $T_i=25^\circ\text{C}$. The tangential momentum accommodation coefficient σ_v and the thermal accommodation coefficient σ_T are set at 0.9. The results are obtained for the specific heat ratio $\gamma=1.4$ and $\text{Pr}=0.7$. Also geometry parameters is taken $\lambda=2$.

A. The flow field

The effect of Knudsen number on slip velocity in the wavy microchannel is shown at Fig. 4. By increasing the Knudsen number, the channel dimensions decrease and approaches to molecular dimensions and the effect of slip velocity would become more and more important.

Moreover, in the convergent regions, the average velocity increases that contributes to a rapid raise in the slip velocity in this region.

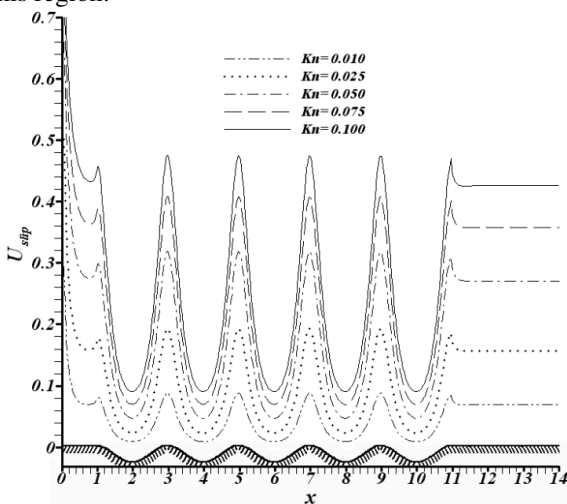


Fig. 4 Variation of slip velocity along the wavy microchannel with Knudsen number $\text{Re}=2$ and $a=0.2$

Fig. 5 compares the velocity profile in different Knudsen numbers and in different cross sections. It schematically shows when rarefaction increases, the slip velocity values become greater. In addition, in each Knudsen number as the fluid approached throttle regions, the slip velocity becomes more considerable because of increasing the average velocity.

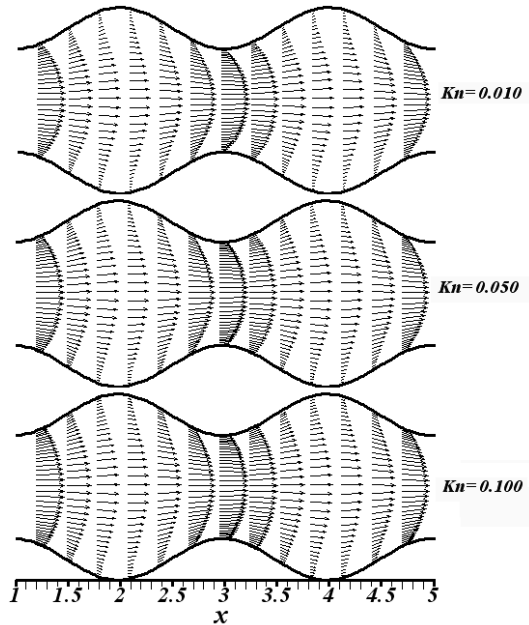


Fig. 5 Schematic illustration of Knudsen number effect on velocity profile at $\text{Re}=2$ and $a=0.2$

The variations of $C_f \cdot \text{Re}$ along the microchannel for various Knudsen numbers in the hydrodynamically/thermally developing region are depicted at Fig. 6. It is evident that there is high friction at the entrance region due to presence of high velocity gradients. However, it rapidly decreases as the flow develops. Moreover, rarefaction has a decreasing effect on the friction factor. This effect can be interpreted mathematically. Eq. (10) shows that $C_f \cdot \text{Re}$ depends on the average velocity and the gradient of tangential velocity. As Knudsen increases, because of a fixed Re we have higher Mach number that results in greater average velocity. In addition, larger Knudsen number decreases the slope of velocity near the wall and this means having lesser tangential velocity gradient. Therefore, in according to the previous explanation, the larger Knudsen number causes the lesser $C_f \cdot \text{Re}$.

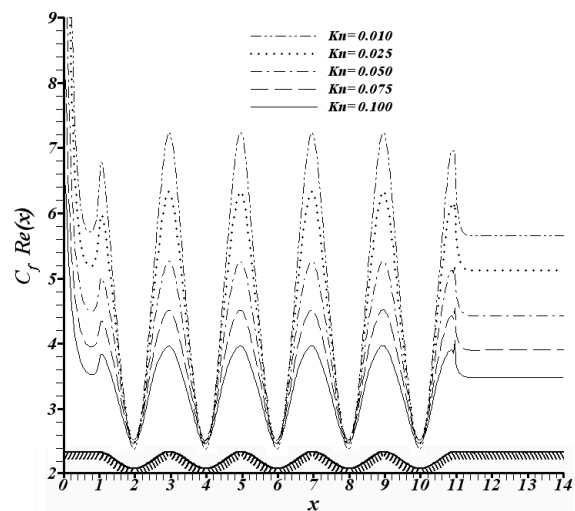


Fig. 6 Variation of $C_f \cdot \text{Re}$ along the wavy microchannel with Knudsen number at $\text{Re}=2$ and $a=0.2$

As it can be observed in Fig. 6, when the fluid flows in the divergent region, $C_f \cdot \text{Re}$ experiences a rapid decrease in the microchannel because of decreasing the average velocity.

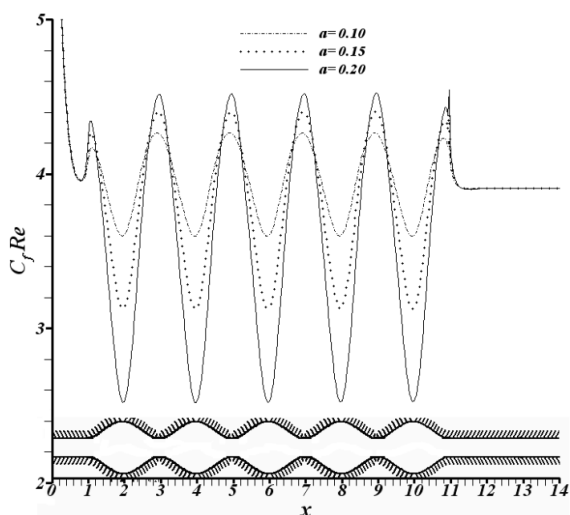


Fig. 7 Variation of $C_f Re$ along the wavy microchannel with geometry at $Re=2$ and $Kn=0.075$

Fig. 7 shows the variation of $C_f Re$ as a function of amplitude of the wave while keeping the Reynolds number and Knudsen number constant. By increasing amplitude of the wave, the fluid flow senses the variation of cross section more.

As it can be seen by increasing amplitude of the wave and subsequently the more decrease in the average gradient of tangential velocity, $C_f Re$ experiences more intense decrease in the divergent region as explained for Fig. 6.

B. The temperature field

The variation of fluid temperature near the wall along the microchannel for various Knudsen numbers is depicted in Fig. 8. As shown, the larger Knudsen numbers, the higher temperature jumps. By decreasing of the channel dimensions, the thickness of the Knudsen number layer increases that bring about further temperature jump. In addition, it is found that this effect is gradually diminishing as the fluid flow approaches the developed region.

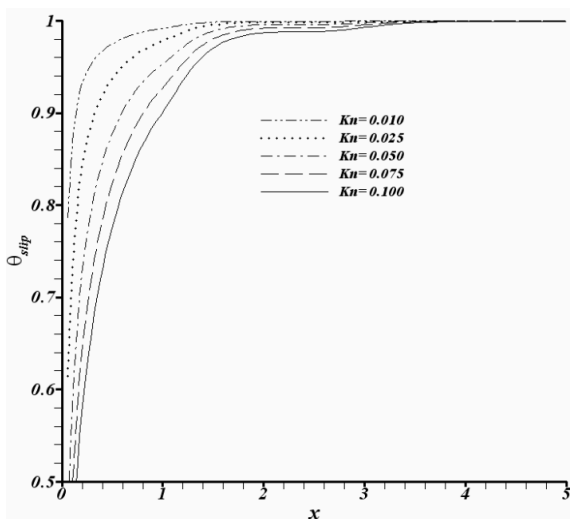


Fig. 8 Variation of slip temperature with Knudsen number along the wavy microchannel at $Re=2$ and $a=0.2$

The effect of Knudsen number on local Nusselt number for hydrodynamically/thermally developing flow in the wavy

microchannel is presented in Fig. 9. As expected, very high heat transfer rate is experienced in the entrance region of the microchannel due to high temperature gradient. As expected also, high heat transfer rate diminishes rapidly as the thermally developing flow approaches the fully developed flow. Because of increasing of the average velocity and especially slip velocity in the convergent regions, there is a jump in the local Nusselt in these regions. Besides, Nusselt number in the microchannel lower as the rarefaction increases. As already sated, when rarefaction increases the temperature jump is intensified. The temperature jump means the absolute difference between the average temperature and wall temperature. So the temperature jump decreases the Nusselt number by increasing the absolute difference of the wall temperature and mean gas temperature.

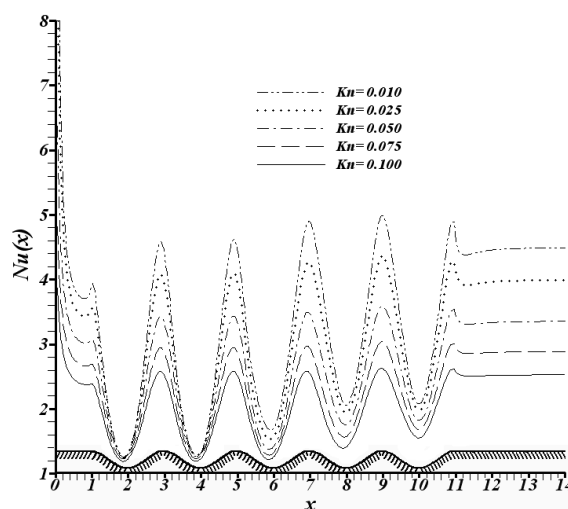


Fig. 9 Variation of local Nusselt number along the wavy microchannel with Knudsen at $Re=2$ and $a=0.2$

Fig. 10 shows the variation of Nusselt number as a function of amplitude of the wave while keeping the Reynolds number and Knudsen number constant. By increasing amplitude of the wave, the fluid flow senses the variation of cross section more. As it can be seen by increasing amplitude of the wave, Nusselt number experiences much larger fall in the divergent region due to decrease in the average velocity.

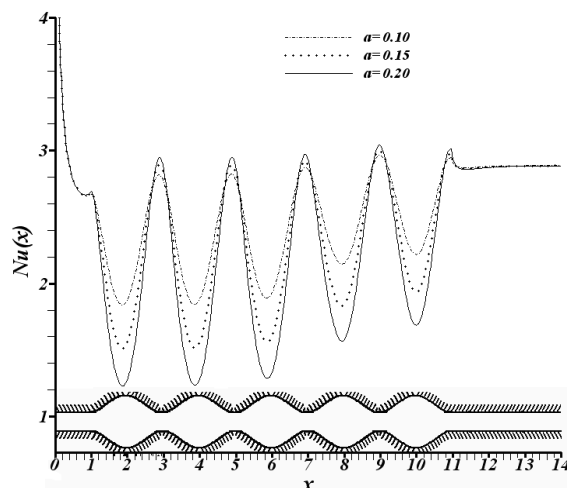


Fig. 10 Variation of local Nusselt number along the wavy microchannel with Knudsen at $Kn=0.075$ and $Re=2$

VIII. CONCLUSION

In this study, the continuum approach with the velocity slip and temperature jump condition at the solid walls is applied to develop the mathematical model of flow phenomenon in the wavy microchannel. These equations are solved by SIMPLE algorithm in curvilinear coordinate. The flow and heat transfer characteristics of laminar incompressible gaseous flow in a wavy microchannel are analyzed.

The effects of Knudsen number and geometry on thermal and hydrodynamic characteristics of flow in the wavy microchannel at constant Reynolds number are illustrated in this work. It is found that the Nusselt number and $C_f \cdot Re$ decrease with Knudsen number. It is also found that $C_f \cdot Re$ and Nusselt numbers experience a rapid jump in the convergent part and this jump is more considerable for lower Knudsen numbers. In addition, the model successfully predicts the growth of temperature jump and slip velocity with Knudsen number at the solid walls. Moreover, by decreasing amplitude of the wave, the variation of Nusselt number and $C_f \cdot Re$ in the wavy region become more intense.

NOMENCLATURE

a	amplitude of the wave (m)
k	thermal conductivity of air (W/m.K)
h	local heat transfer coefficient (W/m ² .K)
J	Jacobian of the coordinate transformation
p	dimensionless pressure
Re	Reynolds number (Re= $\rho u_i L^* / \mu$)
Pr	Prandtl number (Pr = ν / α)
Nu	local Nusselt number
Nu _∞	fully developed Nusselt number
Kn	Knudsen number
Ma	Mach number
Pe	Peclet number
Ec	Eckert number
C _f	skin-friction coefficient
c _p	specific heat (J/kg K)
n	dimensionless normal direction to the wall
s	dimensionless tangential direction to the wall
R	gas constant (J/kg.K)
T	temperature (K)
q''	heat flux
u	dimensionless velocity component in x-direction
v	dimensionless velocity component in y-direction
L*	channel inlet width
x	dimensionless horizontal coordinate
y	dimensionless vertical coordinate

Greek Symbols

a	thermal diffusivity(m ² /s)
λ	surface wavelength (m)
ρ	density of fluid (kg/m ³)
μ	dynamic viscosity (kg/m.s)
γ	ratio of specific heats (c _p /c _v)
λ	molecular mean free path (m)
ν	kinematic viscosity(m ² /s)
σ _T	energy accommodation coefficient
σ _v	momentum accommodation coefficient
θ	dimensionless temperature
ξ	curvilinear horizontal coordinate
η	curvilinear vertical coordinate

τ shear stress

Subscripts

ave	mean value
w	surface conditions
i	inlet conditions
s	fluid property near the wall

Superscript

C	contravariant velocities
tang	tangential direction
*	returns to dimensional parameters

REFERENCES

- [1] Jennifer van Rij, Todd Harman, Timothy Ameal, "The effect of creep flow on two-dimensional isoflux microchannels", International Journal of Thermal Sciences 46 (2007) 1095–1103.
- [2] Lütfullah Kuddusi, Edvin Çetegen, "Thermal and hydrodynamic analysis of gaseous flow in trapezoidal silicon microchannels", International Journal of Thermal Sciences 48 (2009) 353–362.
- [3] Graur IA, Meolans JG, Zeitoun DE "Analytical and numerical description for isothermal gas flows in microchannels", Microfluid Nanofluid 2 (2006) 64–67.
- [4] Jiji LM, "Effect of Rarefaction, Dissipation, and Accommodation Coefficients on Heat Transfer in Micro cylindrical Couette Flow", ASME J. Heat Transfer 130 (2008) 385–393.
- [5] Chen CS, Kuo WJ, "Heat transfer characteristics of gaseous flow in long mini- and microtubes", Numerical Heat Transfer; Part A: Applications 46 (2004) 497–514.
- [6] Larrode FE, Housiadas C, Dreossinos Y, "Slip-flow heat transfer in circular tubes", Int J. Heat and Mass Transfer, 43 (2000) 2669–2680.
- [7] Kavehpour HP, Faghri M, Asako Y, "Effects of compressibility and rarefaction on gaseous flows in microchannels", Numerical Heat Transfer; Part A: Applications 32 (1997) 677–696.
- [8] Cheng RT-S, "Numerical Solution of the Navier-Stokes Equations by the Finite Element Method", Phys. Fluids 15 (1972) 2098–2105.
- [9] Vradsis G, Zalak V, Bentson J, "Simultaneous, variable solutions of the incompressible steady Navier-Stokes equations in general curvilinear coordinate systems", Trans. ASME I: J. Fluids Engng. 114 (1992) 299–305.
- [10] Wang CC, Chen CK, "Forced convection in a wavy-wall channel", International Journal of Heat and Mass Transfer 47 (2004) 3877–3887.
- [11] E.B. Arkilic, K.S. Breuer, M.A. Schmidt, "Gaseous Flow in Microchannels", ASME Application of Microfabrication to Fluid Mechanics 197 (1994) 57–66.
- [12] A. Beskok, G.E. Karniadakis, W. Trimmer, "Rarefaction and compressibility effects in gas microflows", Journal of Fluids Engineering, Transactions of the ASME, 118 (3) (1996) pp. 448–456.
- [13] Kennard EH, "Kinetic theory of gasses", New York: McGraw-Hill (1938).
- [14] Gombosi TI, "Gas kinetic theory", New York: Cambridge University Press (1994).
- [15] Gad-el-Hak M, "The MEMS Handbook", CRC Press LLC, Boca Raton (2002).
- [16] Kandlikar S, Garimella S, Li D, Colin S, King MR (2006), "Heat Transfer And Fluid Flow In Minichannels and Microchannels", Elsevier, Britain.
- [17] Patankar SV, "A calculation procedure for heat, mass and momentum transfer in three-dimensional parabolic flows", Int J Heat Mass Transf 15 (1972) 1787–1806.
- [18] Spalding DB, "A novel finite difference formulation for differential expressions involving both first and second derivatives", Int J Numer Methods Eng 4 (1972) 551–559.
- [19] Hoffman KA, "Computational fluid dynamics for engineers", Engineering Education System, Austin (1989).